A Yeast Mitochondrial Membrane Methyltransferase-like Protein Can Compensate for *oxa*1 Mutations

Claire Lemaire, Florence Guibet-Grandmougin, Diane Angles, Geneviève Dujardin, Nathalie Bonnefoy

THE JOURNAL OF BIOLOGICAL CHEMISTRY
Vol. 279, No. 46, Issue of November 12, pp. 47464–47472, 2004
Printed in U.S.A.

A Yeast Mitochondrial Membrane Methyltransferase-like Protein Can Compensate for *oxa1* Mutations*

Received for publication, April 30, 2004, and in revised form, August 31, 2004
Published, JBC Papers in Press, September 8, 2004, DOI 10.1074/jbc.M404861200

Claire Lemaire, Florence Guibet-Grandmougin, Diane Angles, Geneviève Dujardin, and Nathalie Bonnefoy‡

From the Centre de Génétique Moléculaire, CNRS Gif-sur-Yvette, UPR 2167, Avenue de la Terrasse, 91198 Gif-sur-Yvette Cedex, France

Members of the Oxa1p/Alb3/YidC family mediate the insertion of various organelle or bacterial hydrophobic proteins into membranes. They present at least five transmembrane segments (TM) linked by hydrophilic domains located on both sides of the membrane. To examine how Oxa1p structure relates to its function, we have introduced point mutations and large deletions into various domains of the yeast mitochondrial protein. These mutants allowed us to show the importance of the first TM domain as well as a synergistic interaction between the first loop and the C-terminal tail, which both protrude into the matrix. These mutants also led to the isolation of a high copy suppressor, *OMS1*, which encodes a member of the methyltransferase family. Overexpression of *OMS1* seems to increase the steady-state level of both the mutant and wild-type Oxa1p. We show that Oms1p is a mitochondrial inner membrane protein inserted independently of Oxa1p. Oms1p presents one TM and a N-in C-out topology with the C-terminal domain carrying the methyltransferase-like domain. A conserved motif within this domain is essential for the suppression of *oxa1* mutations. We discuss the possible role of Oms1p on Oxa1p intermembrane space domain.

Mitochondria are organelles that are essential for numerous metabolic reactions, including the oxidative phosphorylations that provide non-photosynthetic eukaryotic cells with their major source of ATP. The mitochondrial inner membrane contains the respiratory chain complexes and ATP synthase as well as numerous other proteins, such as transporters and translocators. This extremely high protein content makes the mitochondrial inner membrane a good model system to study how hydrophobic proteins from different origins can reach their final destination and acquire their proper topology and their assembly partners in a lipid bilayer.

Most of the proteins synthesized in the cytoplasm and imported into the mitochondrial membrane are dependent on the Tom and Tim translocases from the outer and inner membranes (for review see Ref. 1). Other factors are necessary to ensure the correct insertion of the small number of respiratory complex subunits that are encoded by the mitochondrial genome and inserted within the inner membrane. First, at least in *Saccharomyces cerevisiae*, specific translational activators bound to the membrane recognize the 5′-untranslated leaders of most mitochondrial mRNAs and probably contribute to localize mitochondrial translation in the vicinity of the membrane, facilitating subsequent membrane integration of the newly synthetized peptides (2). The modulation of mitochondrial protein synthesis can also promote its coupling with membrane insertion (3). Second, in eukaryotic mitochondria, Oxa1p is an important inner membrane component mediating membrane insertion of mitochondrial proteins and the export of some domains that have to be translocated into the intermembrane space. In particular, Oxa1p could be crucial for the insertion and lateral exit of mildly hydrophobic transmembrane (TM)[1] segments (4) and for the translocation of charged soluble domains (5).

Oxa1p is functionally conserved in higher eukaryotes (6, 7), and the Oxa1p family extends far beyond eukaryotic mitochondria because members are present in both bacteria, such as YidC, and chloroplast (8–10). In the yeast *S. cerevisiae*, the deletion of the *OXA1* gene prevents respiratory growth because it impairs the biogenesis of the three respiratory complexes of dual genetic origin, cytochrome *c* oxidase being the most affected (11, 12). In particular Oxa1p seems essential for the co-translational insertion of Cox2p, which is encoded by the mitochondrial genome and the export of its soluble domain within the intermembrane space (13–16). In *Escherichia coli*, YidC interacts with the Sec system to function as a membrane insertase. In particular, YidC is required for the insertion of ATPase subunits (9, 17–19). In *Arabidopsis* chloroplasts, the Alb3 protein mediates the insertion of the light antenna complexes into the thylakoid membrane (20). The *Chlamydomonas* Alb3 is also required for efficient assembly of photosystem II (21). The Oxa1p, YidC, and Alb3 proteins share modest sequence homology but show a conserved structure with five or six TM segments interrupted with hydrophilic loops located on either side of the membrane (22, 23). YidC contains six TM domains, and both its C and N termini are located in the cytoplasm. In eukaryotes, Oxa1p-type proteins show a N-out C-in topology (24) and five TM domains with a long basic C-terminal tail.

In an effort to analyze the domains of Oxa1p and to examine how its structure relates to its function and the interaction with its substrates, we have introduced point mutations and large deletions into various domains of the protein that are located in the membrane, the intermembrane space, or the matrix. We find that mutating two TM residues specific to the eukaryotic members of the family specifically affects cytochrome *c* oxidase activity. In addition, the two matrix regions of Oxa1p appear dispensable independently but their simultane-

* This work was supported by a research grant from the Association Française contre les Myopathies (to G. D. and N. B.). The costs of publication of this article were defrayed in part by the payment of page charges. This article must therefore be hereby marked "*advertisement*" in accordance with 18 U.S.C. Section 1734 solely to indicate this fact.

‡ To whom correspondence should be addressed. Tel.: 33-1-69-82-31-75; Fax: 33-1-69-82-31-60; E-mail: bonnefoy@cgm.cnrs-gif.fr.

[1] The abbreviations used are: TM, transmembrane; ORF, open reading frame; L, loop.

ous removal causes a severe respiratory deficiency. These mutants led to the isolation of a high copy suppressor, *OMS1*, which encodes a mitochondrial inner membrane protein of the methyltransferase family. The suppression mechanism has been investigated, and its functional implications are discussed.

EXPERIMENTAL PROCEDURES

1. Strains, Media, and Genetic Techniques—All of the strains were derived from the W303 nuclear background *MATα ade2–1 ura3–1 his3–11,15 trp1–1 leu2–3,112 can1–100*. CW04 is the wild-type strain (11), NBT1 is the *oxa1*::*LEU2* strain (6), and NBT3 is the *oxa1*Δ::*URA3* strain (12). The thermosensitive strain (*oxa1-ts1402*) (25) in which leucine 240 of Oxa1p is substituted by serine was constructed by K. Hell and R. A. Stuart. The Δ*mba1* strain was from J. M. Herrmann. The Δ*afg3* strain (*afg3*::*HIS3*) was from A. Tzagoloff. Media and genetic techniques were as described previously (11).

2. Subcloning and Site-directed Mutagenesis—The 3-kb SacI KpnI fragment containing the *OXA1* ORF was subcloned into the same sites of pRS416, a centromeric plasmid (26), to yield pNB160. Mutant DNA fragments were obtained by two-step PCR as described previously (27). In mutant WW→AA, codons 128–129 (TGG TGG) were replaced by GCA GCT, creating both a PstI and a PvuII site with the flanking wild-type nucleotide. Codon 140 (CGA) encoding arginine was changed to GCA (alanine), creating an HpaI site, or to GAA (glutamate). Codons 332 and 353 were changed from AAA (lysine) to the stop codon TAA, and codon 376 was altered from TTA (leucine) to GTA. Simultaneously, a NcoI, HpaI, or SpeI site was created downstream stop codon 332, 353, or 376, respectively. Deletion of the 43 codons of L1 created an HpaI site. Deletion of L2 or TM4–5 removed 25 and 33 codons, respectively. Mutant *OXA1* fragments were subcloned into pNB160 using various restriction sites located throughout the *OXA1* ORF. All of the plasmids generated were verified by sequencing the regions coming from PCR amplification and the cloning junctions. For some mutants, the SacI KpnI 3-kb fragment was subcloned into the high copy *URA3* vector YEp352 (28).

3. Homologous Recombination—The *oxa1* mutations were integrated into the genome. However, as the different C-terminal truncations showed a similar phenotype on plasmid, only the largest one, K332*, was chosen for homologous integration into the yeast genome. The resulting *oxa1* mutation was identical to that carried by the *oxa1*$^{1-331}$ mutant used by Szyrach *et al.* (16). SacI KpnI linear fragments containing the mutated *OXA1* genes were mixed with a circular LEU2 vector (Yep351) (28) and used to transform the *oxa1*Δ::*URA3* strain NBT3. [Leu$^+$] transformants were selected and replica-plated onto medium containing 5-fluoro-orotic acid, which is toxic in [Ura$^+$] cells, to screen for [Leu$^+$] [Ura$^-$] clones. The phenotype of each recombinant strain was similar to that of a Δ*oxa1* strain expressing the corresponding mutant gene from a centromeric plasmid. The structure of the *OXA1* locus was confirmed by PCR analysis and sequencing for each strain.

4. Library Screening—Mutant WW→AA was transformed with a high copy library constructed by F. Lacroute into the *URA3* 2 μ vector pFL44L. [Ura$^+$] clones were selected and replica-plated onto glycerol medium at 36 °C. Total yeast genomic DNA was extracted from three co-segregating slow-growing [Gly$^+$] clones and used to transform *E. coli* cells to recover the plasmids. Molecular analysis by restriction enzymes and sequencing showed that two plasmids were carrying truncations of *OXA1* itself and that the last one, pNB212, contained a new chromosome IV insert carrying the *YDR316w*/*OMS1* gene.

5. Mutagenesis of OMS1—A 1.76-kb SacI SphI fragment containing *OMS1* was excised from a deletion derivative of pNB212 (Fig. 3*A*, *line 6*) and subcloned into the same sites of vector Yep352 (28). This new plasmid, pNB229, still carried the suppressor activity and contained two XbaI sites 554 bp apart surrounding the third methyltransferase motif coding region of *OMS1* (*motif II*, see Fig. 6*A*). A PCR primer was designed that contained the first XbaI site and a modified motif II coding region. Codon 326, which was coding for aspartate, was changed from GAT to GCA (alanine). In addition, the following codon was altered from ACT (threonine) to TCT (serine), which allowed the creation of a NsiI while still coding a hydroxylated amino acid at position 327. Previous studies have shown that this position did not matter for the methyltransferase activity (29). A mutated version of the XbaI 554-bp fragment was generated by PCR amplification and subcloned in-frame into the XbaI sites of pNB229 to replace the wild-type fragment. In this new plasmid, pNB230, the expected mutation was verified by the presence of the NsiI site followed by sequencing of the cloned XbaI fragment and junctions.

6. Epitope Tagging and Deletion of OMS1—Oms1p was tagged by fusing the c-Myc epitope at the last residue (amino acid 471) using PCR fragments containing 41 and 43 bp homologous to *OMS1* on the 5′ and 3′ sides of the c-*myc*-*HIS3* cassette (30). The PCR fragment was introduced into a wild-type strain, either untransformed or carrying the pNB212, pNB229, or pNB230 *OMS1* plasmids to integrate the c-Myc construct either in the yeast genome or in the plasmid. Correct integration of the tag in the *OMS1* ORF was confirmed both on genomic and on plasmidic DNA by PCR amplification and sequencing. The genomic version of *OMS1* was deleted using a *Kan*^{R} PCR fragment that contains 50 bp of the *OMS1*-flanking regions on each side. The integration was confirmed by PCR analysis of the genomic DNA, and the [G418^R] phenotype was shown to segregate 2:2 and to correlate with the presence of the disrupted version of *OMS1*.

7. Mitochondria Purification, Western Blotting, Determination of Respiratory Complex Activities, and ^{35}S Labeling—Cells were grown either in complete or minimal galactose medium, and mitochondria were purified as described previously (31). Swelling and protease K treatment of mitochondria were carried out as described previously (32). Mitochondria were analyzed by SDS-PAGE followed by blotting onto a nitrocellulose membrane and hybridization with various antibodies: anti-Cox2p and anti-porin (Molecular Probes); anti-cytochrome c_1 (raised in our laboratory against a fusion protein ProA-apocytochrome c_1 expressed in *E. coli*); anti-Atp2p and anti-Atp4p (J. Velours); anti-c-Myc (J. M. Galan); and anti-Arg8p (T. D. Fox). Immunodetection was carried out using the standard chemiluminescence method. To measure the cytochrome *c* oxidase activity, the oxidation of previously reduced cytochrome *c* was followed spectrophotometrically at 550 nm according to Pajot (33). Ubiquinol cytochrome *c* oxidase activity (*bc1* activity) was measured according to Brasseur *et al.* (34). Oligomycin-sensitive ATPase activity was measured by colorimetric determination of inorganic phosphate released from ATP according to Spannagel *et al.* (35). ^{35}S labeling of mitochondrial proteins was performed on whole cells in the presence of cycloheximide that specifically blocks cytoplasmic translation as described by Lemaire *et al.* (36).

RESULTS

1. Mutations in Different Domains of Oxa1p Lead to Different Respiratory Growth Phenotypes—To investigate the function of the different domains of Oxa1p, mutations were created in the gene on a centromeric plasmid using a PCR-based site-directed mutagenesis strategy and then integrated at the chromosomal *OXA1 locus* (Fig. 1*A*). First, missense mutations were introduced in or close to the sequences encoding the first hydrophobic segment TM1. The pair of tryptophans 128–129, specific to eukaryotic Oxa1p/Alb3p-type sequences, was changed to a pair of alanines (WW→AA), whereas the basic arginine 140 adjacent to TM1 was substituted by either the neutral alanine (R140A) or the acidic glutamate residue (R140E). Second, nonsense mutations were placed in the 3′ end of *OXA1* to generate three different truncations of the C-terminal tail of Oxa1p (K332*, K353*, and K376*). Third, large deletions were made within loop 1 (ΔL1) or loop 2 (ΔL2) or by fusing loop 3 to the C-terminal tail to eliminate TM4 and TM5 (ΔTM4–5).

The phenotypes of these various mutants were analyzed on respiratory media containing different non-fermentable carbon sources (ethanol/glycerol/lactate), which cannot sustain growth of the null mutant Δ*oxa1* (Fig. 1*B*). The missense mutations WW→AA in TM1 led to a very strict thermosensitive and slightly cryosensitive phenotype on non-fermentable medium, whereas modification of Arg^{140} (R→E, R→A) only conferred a cryosensitive phenotype on lactate medium. Similar to the Δ*oxa1* mutant, ΔL2 and ΔTM4–5 did not grow at all on these non-fermentable media. ΔL1 and the truncations of the C-terminal tail of Oxa1p were indistinguishable from the wild type at 28 °C, although K332* showed some weak sensitivity to either high or low temperatures. It was striking that ΔL1 and K332* gave mild phenotypes while deleting such large matrix parts of the protein, so we constructed a double mutant ΔL1-K332* by combining both matrix mutations. This ΔL1-K332* mutant does not grow on non-fermentable medium.

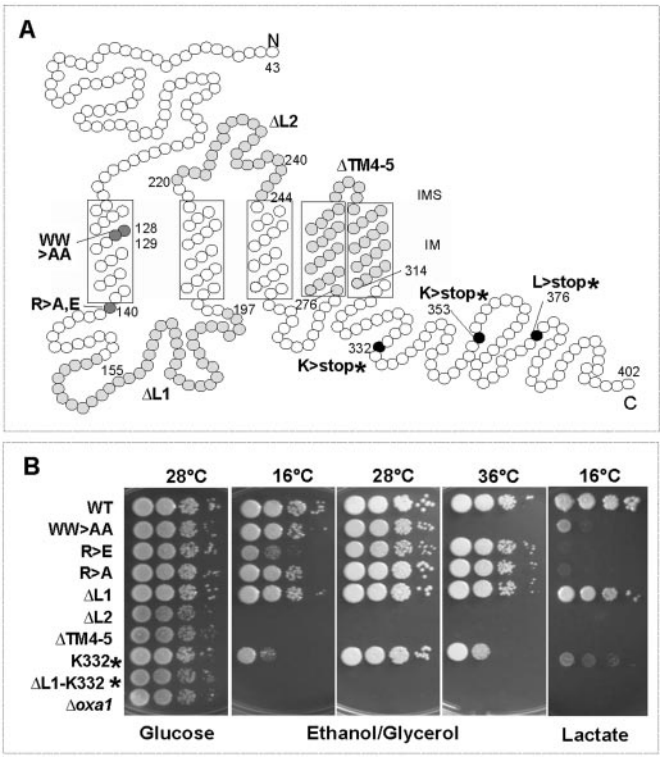

FIG. 1. **Oxa1p mutant structures and growth phenotypes.** *A*, a putative topology of Oxa1p is presented with its five TM segments within the inner membrane of mitochondria (*IM*). The N terminus (*N*) is in the intermembrane space (*IMS*) and the C terminus (*C*) in the matrix. Each *circle* corresponds to an amino acid, starting from position 43, as the Oxa1p presequence is expected to be cleaved around this position (24). Residues altered to non-sense mutations in the C-terminal tail of Oxa1p are depicted in *black*, whereas missense mutations at positions 128–129 and 140 are shown in *dark gray*. Residues deleted are filled in *light gray*. The position of the substitutions or the inclusive limits of the deletions are indicated. Names of the various mutants are given in *boldface letters*. *B*, 10-fold serial cell dilutions of the integrated mutants were spotted onto complete medium containing various carbon sources and incubated at different temperatures for 2–22 days depending on the temperature or the carbon source. Glucose is a fermentable carbon source, whereas glycerol, ethanol, and lactate are non-fermentable.

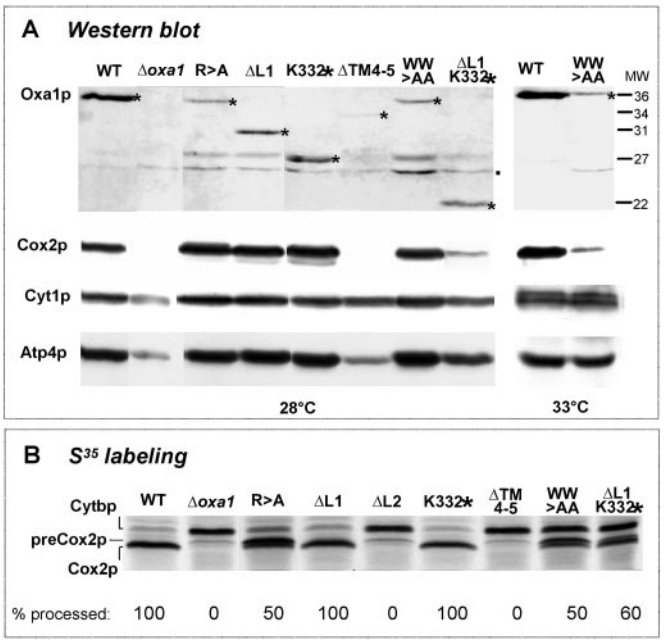

FIG. 2. **Biochemical analysis of the mutants.** *A*, mitochondria were extracted from cells grown at 28 (*left panel*) or 33 °C (*right panel*). Mitochondrial proteins were run on a 12% acrylamide gel before Western blotting with the anti-Oxa1p antibody and with anti-Cox2p, anti-Cyt1p, and anti-Atp4p antibodies. *Stars* indicate the band corresponding to the Oxa1p variants in each lane, and the dot shows a nonspecific signal present even in the Δ*oxa1* strain. Molecular masses are given on the *right side*. *B*, cells were grown at 28 °C and labeled with [^{35}S]methionine and [^{35}S]cysteine in the presence of cycloheximide for 20 min. The newly translated mitochondrial products were separated on a 16% acrylamide-0.5% bis gel (51) before exposure. The level of processed Cox2p has been determined for each mutant using the ImageQuant program (Molecular Dynamics) and is given as an average percentage of wild type.

2. Effect of the Various Mutations on the Steady-state Level of Oxa1p and on the Assembly of the Respiratory Complexes—The mutants were subjected to biochemical analysis to determine both the steady state-level and size of the Oxa1p variants and the effect on respiratory complex biogenesis. With the exception of ΔL2 in which the Oxa1p protein was repeatedly undetectable, the mutated Oxa1p could be detected in purified mitochondrial extracts in all of the other mutants but always in lower steady-state levels than in the wild type (Fig. 2*A*). We could find no correlation between the levels of Oxa1p variants and either the nature of the mutation or the strength of the phenotype. Rather Oxa1p levels seemed extremely sensitive to any type of mutation. This could be due to the fact that Oxa1p is known to facilitate its own insertion (37) and is very sensitive to proteases (38). For all of the mutants, the observed size of the Oxa1p variants was compatible with the predicted size. Strikingly, the level of the Oxa1p variant observed in WW→AA was similar whether it was at permissive or restrictive temperature, suggesting that the mutated protein activity rather than its accumulation is affected by high temperature. In addition, the level of the ΔL1-K332* was similar to that of the two single mutants, showing that the large double deletion did not further destabilize Oxa1p.

In absence of Oxa1p, the N-tail translocation of the Cox2p precursor into the intermembrane space is blocked (25). Consequently, the maturation of pre-Cox2p cannot occur and the unprocessed precursor is rapidly degraded. The new mutants were subjected to ^{35}S labeling of the mitochondrial proteins at 28 °C (Fig. 2*B*). As usual, in this strain background, the cytochrome *b* labeling signal was stronger when Oxa1p function was affected.[2] Whereas Cox2p was entirely matured in ΔL1 and K332*, ΔL2 and ΔTM4–5 behaved like Δ*oxa1* mutants. Interestingly, R→A and WW→AA, which showed wild-type growth on non-fermentable carbon source at 28 °C, were partly defective in pre-Cox2p processing, similarly to ΔL1-K332*, which exhibited a strong respiratory-deficient phenotype. This finding suggests that the respiratory growth deficiency of ΔL1-K332* was due to respiratory chain biogenesis defect that was distinct from pre-Cox2p membrane insertion.

The effect of these *oxa1* mutations on respiratory complex assembly was further analyzed by combining immunodetection experiments and respiratory enzyme activity measurements on purified mitochondria. First, Western blot analysis of the steady-state level of three representative subunits of cytochrome *c* oxidase (Cox2p), complex *bc1* (Cyt1p), and ATPase (Atp4p) was performed for all of the mutants (Fig. 2*A*). At 28 °C, R→A, ΔL1, K332*, and WW→AA behaved similarly to the wild type, whereas ΔTM4–5 was similar to the Δ*oxa1* mutant. ΔL1-K332* grown at 28 °C and WW→AA grown at a restrictive temperature showed an intermediate phenotype. Second, respiratory enzyme activity measurements were performed for the two latter mutants (Table I). ΔL1-K332* exhibited a dramatic 90% decrease in cytochrome *c* oxidase activity

[2] C. Lemaire, unpublished data.

TABLE I
Respiratory chain enzyme activity in some oxa1 mutants

Mitochondria were purified from cells grown in complete galactose medium at the indicated temperature, 28 or 33 °C. However, activities were all recorded at 28 °C. III, ubiquinol cytochrome *c* oxidoreductase activity was in the wild type of 514 or 538 nmol of reduced cytochrome *c*/min/mg protein for cells grown at 28 or 33 °C respectively. IV, cytochrome *c* oxidase activity was in the wild type of 371 or 390 nmol of oxidized cytochrome *c*/min/mg protein for cells grown at 28 or 33 °C. V, ATPase activity was in the wild type of 1.7 or 1.9 μmol of ATP hydrolyzed/min/mg protein for cells grown at 28 or 33 °C. Mutant activities are expressed as the percentage of wild-type absolute activities. All of the values were a mean of 3–5 repeats. Means ± S.D. were comprised of 10 and 20% of the measurements.

Growth temperature	Strain	Activities at 28 °C		
		III	IV	V
°C				
28	WT	100	100	100
	WW→AA	104	88	94
	Δ L1-K332*	**35**	**10**	**50**
	Δ*oxa1*	19	0	16
33	WT	100	100	100
	WW>AA	109	**17**	84

and at least a 50% decrease in *bc1* and ATPase activities. At restrictive temperature, WW→AA presented a specific defect of cytochrome *c* oxidase, whereas the ATPase and the *bc1* activities were nearly wild type. Thus, all of the biochemical analyses showed that ΔL1-K332* has a pleiotropic phenotype that reflects the requirement of the matrix domains for the biogenesis of the three respiratory complexes, whereas WW→AA specifically affects cytochrome *c* oxidase formation at high temperature.

3. YDR316w/OMS1 Is a High Copy Suppressor of Partial oxa1 Defects That Genetically Interacts with OXA1—Contrary to the Δ*oxa1* mutant, WW→AA presented spontaneous reversion events of the respiratory deficiency at 36 °C and thus appeared less stringent than Δ*oxa1*. This led us to search for high copy suppressors of WW→AA, even though no high copy suppressors of Δ*oxa1* had ever been isolated. A genomic library cloned in a high copy vector was introduced into WW→AA cells, and colonies presenting a slow growth phenotype on non-fermentable carbon sources were further analyzed. One of them contained a plasmid carrying a 3.9-kb fragment of chromosome IV that conferred suppression after re-transformation of both the original mutant WW→AA and the ΔL1-K332* mutant but only at 28 °C for ΔL1-K332* (Fig. 3*A* and data not shown). This 3.9-kb fragment contained two entire ORFs, *YDR316w* and *IPK1*/*YDR315c*, together with the 5′ region of *YDR314c*. Subcloning and disruption showed that the gene responsible for the suppression was *YDR316w*, an ORF of unknown function, that we called *OMS1* for "*Oxa1* Multicopy Suppressor" (Fig. 3*A*).

In theory, Oms1p could compensate only for all/some *oxa1* deficiencies or it could generally improve the non-fermentable growth efficiency of many conditional respiratory mutants. To decide between these possibilities, we determined the allele specificity of the suppression. Several *oxa1* mutants were transformed with the plasmid carrying *OMS1* and tested for growth on glycerol medium at 28 or 36 °C (data not shown). Whereas Δ*oxa1*, ΔL2, or ΔTM4–5 clearly was not suppressed, the mutant *oxa1-ts1402* corresponding to a thermosensitive substitution of leucine to serine (25) was suppressed similarly to WW→AA and ΔL1-K332* (data not shown). Mitochondria were purified from the ΔL1-K332* transformants carrying the *OMS1* plasmid, and Western blot analysis revealed that overexpression of *OMS1* slightly increased the steady-state level of Cox2p (Fig. 3*B*). To analyze the gene specificity of the suppression, we also transformed various nuclear or mitochondrial mutants showing either thermosensitive or leaky respiratory phenotypes. We found that the Δ*mba1* (39), Δ*nam1* (40), *cox2–10* (41), and *cbs2–223* (42) mutants were not suppressed (data not shown). Thus, the multicopy suppressor phenotype of *OMS1* is specific to some of the alleles of *OXA1*.

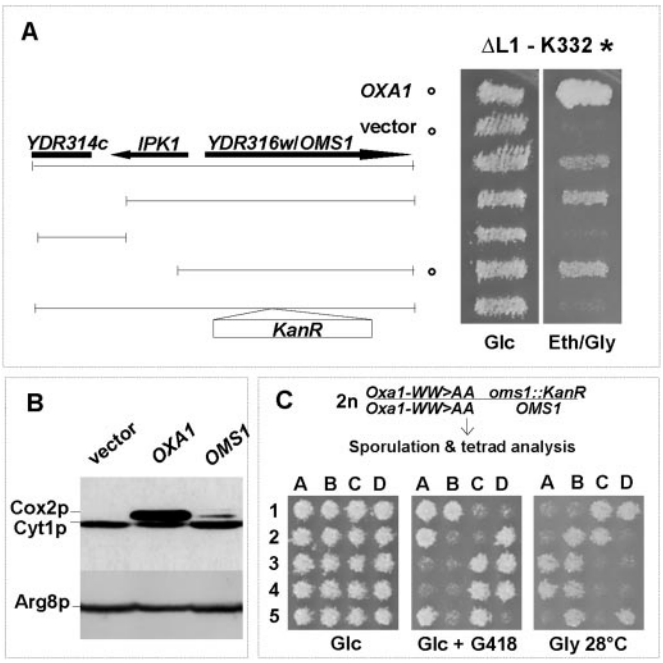

FIG. 3. **Identification and phenotype of a high copy suppressor of *oxa1* mutants.** *A*, ΔL1-K332* cells transformed with the indicated constructs carried by the vector pFL44L were patched on minimal glucose medium lacking uracil (*Glc*) and replica-plated onto a non-fermentable carbon source (ethanol-glycerol). The plates were incubated for 4 days. The first patch corresponds to cells transformed with the wild-type *OXA1* gene carried by pFL44L, and cells from the second patch contain the empty vector. The third patch corresponds to plasmid pNB212 carrying the chromosome IV insert containing the suppressor gene *OMS1*. The *arrows* show the direction of transcription of the different ORFs. The following patches correspond to deletion derivatives of pNB212. The white Kan^R box represents the marker gene conferring resistance to the G418 drug, inserted in the BstEII site at the very beginning of the *OMS1* ORF on plasmid pNB212. The transformants analyzed in *B* are marked with a *circle*. *B*, mitochondrial proteins of the indicated transformants from *A* (vector or expressing high copy of *OXA1* or *OMS1*) were separated on a 12% gel, blotted, and hybridized to the anti-Cox2p and anti-Arg8p antibodies. The Cyt1p signal corresponds to the direct detection of heme *c* chemiluminescence (52). *C*, a diploid homozygous for the thermosensitive *oxa1* allele encoding Oxa1p-WW→AA and heterozygous for the deletion of *OMS1* was subjected to sporulation, and asci were microdissected. Growth of the spores was compared on complete glucose medium supplemented (*Glc + G418*) or not (*Glc*) with the G418 antibiotic that selects for Δ*oms1* and on non-fermentable glycerol medium (*Gly 28 °C*). *Numbers 1–5* refer to five different tetrads. *Letters A* through *D* indicate the four sister spores. All of the 30 tetrads obtained showed identical results.

To study the function of Oms1p, we deleted the gene. The doubling time of the Δ*oms1* cells was slightly longer than that of the isogenic wild-type cells grown in liquid glycerol medium (4 h instead of 2 h 30 min for the wild type at 28 °C). No synergistic growth defect was detected when Δ*oms1* was combined with Δ*oxa1*. However, a strong interaction was observed in a WW→AA thermosensitive background, since the combination of the WW→AA and Δ*oms1* mutations prevented growth on non-fermentable medium already at 28 °C (Fig. 3*C*) and not only at 36 °C as in the WW→AA single mutant (Fig. 1*B*). This growth defect at 28 °C was complemented by the introduction of the *OMS1* plasmid (data not shown). Thus, the absence of Oms1p appears only mildly deleterious for respiration except when combined with a specific *oxa1* mutation.

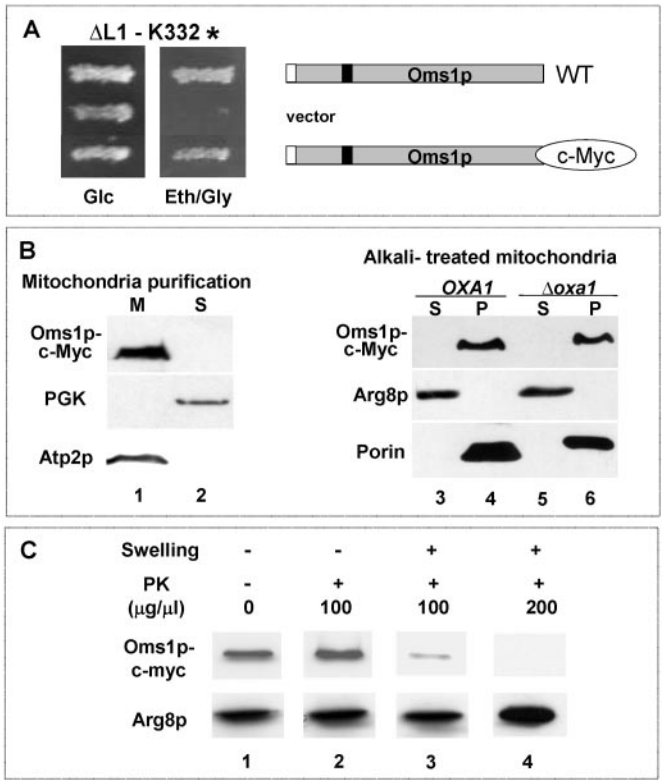

FIG. 4. **Mitochondrial sublocalization and topology of Oms1p.** *A*, ΔL1-K332* cells were transformed with the empty vector pFL44L, the *OMS1* plasmid pNB212, or its c-Myc tag derivative. Transformants were patched on glucose minimal medium before replica-plating onto non-fermentable medium containing ethanol and glycerol and incubated for 4 days at 28 °C. *B*, *left panel*, mitochondrial (*lane 1*) and cytosolic (*lane 2*) protein fractions of a Oms1p-c-Myc-tagged strain were separated and blotted with anti-c-Myc antibody as well as control antibodies recognizing known cytosolic phosphoglycerate kinase (*PGK*) or mitochondrial (Atp2p) markers. *Right panel*, mitochondrial proteins from Osm1p-c-Myc cells containing either the wild type Oxa1p (*OXA1*, *lanes 3* and *4*) or devoid of Oxa1p (Δ*oxa1*, *lanes 5* and *6*) were purified and alkali-treated to separate the soluble proteins recovered in the supernatant (*S*) from the integral membrane proteins that stayed in the pellet (*P*). The different samples were analyzed by Western blotting using the anti-c-Myc antibody and control antibodies specific either to a soluble mitochondrial matrix protein (Arg8p) or an integral mitochondrial membrane protein (Porin). *C*, mitochondrial proteins (*lane 1*) extracted from Oms1p-c-Myc cells were treated with proteinase K (*PK*) before (*lane 2*) or after (*lanes 3* and *4*) swelling to rupture the outer membrane while keeping the inner membrane intact. The three different extracts were blotted with the anti-c-Myc antibody or a control antibody recognizing the matrix protein Arg8p.

4. OMS1 Encodes an Integral Inner Mitochondrial Membrane Protein Inserted Independently of Oxa1p with a N-in C-out Orientation—Oms1p is a 471-residue protein that contains two domains separated by a predicted TM helix starting around residue 108. The large C-terminal domain shows homologies with a large number of eukaryotic and prokaryotic proteins from the methyltransferase family (43). The shorter N-terminal domain presents a possible mitochondrial targeting presequence followed by a region devoid of homology to any protein of known function in the data base. Strong homologs of Oms1p that also exhibit a predicted TM segment upstream of their methyltransferase-type domain appear to be present only in other fungi (data not shown).

To determine whether Oms1p was located in the mitochondria, we generated a strain where the genomic wild-type *OMS1* gene was fused just before the stop codon to the c-Myc epitope. As a control, this tagged derivative was cloned on a high copy plasmid and this construction was still able to suppress the growth defect of the ΔL1-K332* (Fig. 4*A*). Purified mitochondria from the tagged Oms1p-c-Myc strain as well as the post-mitochondrial supernatant were probed with antibodies recognizing the c-Myc epitope, the cytosolic phosphoglycerate kinase, or the mitochondrial protein Atp2p (Fig. 4*B*). Atp2p and c-Myc signals were recovered only in the mitochondrial fraction (*lane 1*), whereas phosphoglycerate kinase was found only in the post-mitochondrial supernatant (*lane 2*), showing that Oms1p-c-Myc is targeted to mitochondria.

Oms1p is predicted to span the membrane once. To test whether Oms1p-c-Myc was associated or not with mitochondrial membranes, we "alkali"-treated purified mitochondria from tagged cells to extract all of the non-integral membrane proteins. As shown in Fig. 4*B* (*lanes 3* and *4*), Oms1p-c-Myc is found in the pellet fraction, similarly to the outer membrane porin and contrary to the matrix protein Arg8p. Thus, Oms1p is an integral mitochondrial membrane protein. The addition of proteinase K to intact mitochondria did not degrade the Oms1p-c-Myc protein or modify its mobility, showing that Oms1p does not span the outer membrane but instead is located in the inner membrane (Fig. 4*C*, *lane 2*). To determine the topology of Oms1p, osmotic swelling was performed on Oms1p-c-Myc mitochondria in the presence of protease to digest all of the outer membrane and intermembrane space proteins. Depending on the concentration of proteinase K used, the protease treatment partially or completely eliminated the c-Myc epitope attached to the C terminus of Oms1p (Fig. 4*C*, *lanes 3* and *4*), whereas the matrix protein Arg8p remained protected, showing that Oms1p C terminus is located in the intermembrane space.

Because Oxa1p is involved in the membrane insertion of various mitochondrial proteins, it could be required for the proper anchoring of Oms1p into the membrane. This would explain why the over production of Oms1p cannot compensate for the complete absence of Oxa1p. To determine whether Oms1p was still associated with the membrane fraction in the absence of Oxa1p, we isolated mitochondria from a tagged Oms1p-c-Myc strain lacking Oxa1p. We found that similar amounts of Oms1p-c-Myc accumulated in the mitochondria and remained associated with the pellet upon alkali treatment (Fig. 4*B*, *lanes 5* and *6*) in the presence or absence of Oxa1p. This showed that proper insertion of Oms1p-c-Myc is independent of Oxa1p function.

5. OMS1 Overexpression Appears to Increase the Steady-state Level of Both the Mutant and Wild-type Oxa1p—Reciprocally, Oms1p could be required to stabilize mutant and/or wild-type Oxa1p. To test this hypothesis, we extracted mitochondrial proteins from a wild type and a Δ*oxa1* strain as well as from ΔL1-K332* cells transformed with a control vector (*lane 5*), a plasmid overproducing Oms1p-c-Myc (*lane 4*) or Oxa1p (*lane 3*). The level of the wild-type and mutant Oxa1p was analyzed in the extracts (Fig. 5*A*). First, the levels of both the wild-type Oxa1p and the Oxa1p-ΔL1-K332* were increased by 3-fold compared with Arg8p levels when the wild-type Oxa1p was overproduced (*lane 3* compared with *lanes 1* and *5*). Second, the mutant ΔL1-K332* protein level was also 4-fold higher compared with Arg8p levels when *OMS1* was overexpressed (*lane 4* compared with *lane 5*), showing that an overexpression of *OMS1*, similar to the overexpression of the wild-type *OXA1* gene, can increase the steady-state level of the mutant Oxa1p.

It was tempting to hypothesize that this increase in the ΔL1-K332* steady-state level by Oms1p could account for the suppression. In this case, direct overexpression of the mutated *oxa1* genes from a high copy plasmid would be predicted to compensate for the deletion of *OXA1*. We found that the ΔL1-K332* and WW→AA mutants could compensate for *OXA1*

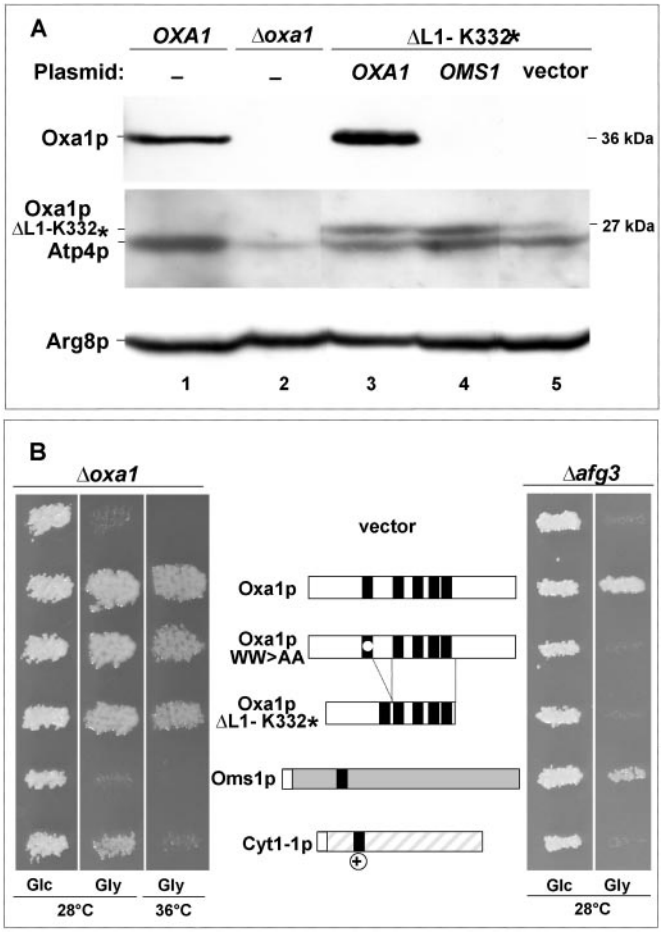

FIG. 5. **Interaction between Oms1p and Oxa1p.** *A*, ΔL1-K332* mutant cells were transformed with plasmids overproducing Oms1p or Oxa1p or with the empty control vector. Mitochondria were purified from the transformants and from wild-type and Δ*oxa1* controls, and mitochondrial proteins were analyzed by Western blotting using the anti-Oxa1p, anti-Atp4p, and anti-Arg8p antibodies. The *two upper panels* correspond to different exposures and different regions of the same membrane obtained from the hybridization experiment with the anti-Oxa1p antibody. Band density values were measured using the ImageQuant program. *B*, the wild type, WW→AA, or ΔL1-K332* versions of the *OXA1* gene were cloned on a high copy vector. The resulting plasmids as well as plasmids overexpressing *OMS1* or the *CYT1-1* dominant suppressor known to compensate for Δ*oxa1* mutants (46) were transformed in the Δ*oxa1* and in the Δ*afg3* mutant together with a control vector. Growth of the transformants on glycerol medium was analyzed at 28 and 36 °C. Glycerol plates were incubated for 5 (Δ*oxa1* mutants) or 9 days (Δ*afg3* mutants).

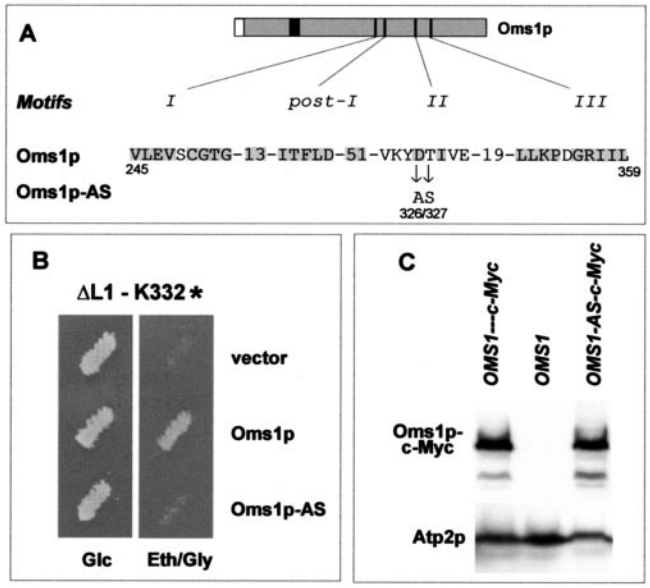

FIG. 6. **Involvement of Oms1p methyltransferase domain in the suppression of *oxa1*-ΔL1-K332*.** *A*, Oms1p is depicted with its four conserved methyltransferase motifs, I, post-I, II, and III (*white bars*). The sequence of the motifs is given in the *one-letter code*, and the *numbers* refer to the number of residues in between the motifs. Residues or spaces are *boxed* in *gray* when they fulfill the consensus found by Niewmierzycka and Clarke (43). In the Oms1p-AS variant, the widely conserved Asp^{326} and the loosely conserved Thr^{237} have been modified to Ala and Ser respectively. B, high copy plasmids producing the wild-type Oms1p or the mutant version Oms1p-AS as well as the control vector Yep352 have been transformed into the ΔL1-K332* mutant. Transformants were patched on selective glucose medium (*Glc*), replica-plated onto non-fermentable plates (*Eth/Gly*), and incubated at 28 °C for 4 days. *C*, the ΔL1-K332* mutant was transformed with plasmids overexpressing either the untagged *OMS1* gene or c-Myc-tagged versions of the wild type (*OMS1-c-Myc*) or mutant gene (*OMS1-AS-c-Myc*). Purified mitochondrial proteins were analyzed by Western blotting using an anti-c-Myc or anti-Atp2p antibody.

deletion when expressed from a high copy vector, even at 36 °C (Fig. 5*B*).

In a similar way, the overexpression of *OMS1* could act on the wild-type Oxa1p. It is known that overexpression of *OXA1* suppresses the respiratory defect due to the absence of Afg3p, a protease facing the matrix side of mitochondria (44, 45). Thus, we transformed the *OMS1* plasmid in the Δ*afg3* mutant and observed that the Δ*afg3* respiratory deficiency is clearly compensated by overexpression of *OMS1* (Fig. 5*B*). This finding suggests that the suppression of Δ*afg3* mediated by high copy of *OMS1* occurs through stabilization of the wild-type Oxa1p. Overproduction of the Oxa1p variants WW→AA or ΔL1-K332* or of the *CYT1-1* suppressor of the *OXA1* deletion (46) could not overcome the respiratory deficiency of Δ*afg3* cells. Taken together, our results indicate that overproduction of Oms1p affects the accumulation of both wild-type and mutant Oxa1p.

6. A Point Mutation in a Conserved Methyltransferase Motif Abolishes the Suppression of oxa1 Mutations—Oms1p belongs to the family of yeast methyltransferases based on its good match with the four typical motifs conserved in a large number of these enzymes (Fig. 6*A*) (43). Thus, it was of interest to determine whether the methyltransferase activity of Oms1p was involved in the suppression. However, to be conclusive, a mutagenic analysis should not lower Oms1p steady-state level because Oms1p-mediated suppression functions only as high dosage.

In rat guanidinoacetate methyltransferase, a widely conserved aspartate residue in the third conserved motif (motif II) has been shown to be crucial for the activity of the enzyme. Mutation into glutamate substantially lowered the activity, whereas mutation into alanine led to inactivation (29). In addition, neither the secondary and tertiary structures of the enzyme nor its stability were affected. It was also shown that conservative change of the residues flanking the aspartate did not affect either the activity or stability of the enzyme (29).

We introduced by PCR-mediated mutagenesis a mutation in Oms1p motif II (Fig. 6*A*). The aspartate was changed to alanine, and for convenience, the threonine adjacent to the aspartate was changed to serine, *i.e.* a conservative change. The mutant gene was cloned on a high copy plasmid and transformed into the ΔL1-K332* mutant together with the wild-type control plasmid. Whereas the suppression was clearly seen in 4 days with wild-type plasmid, the mutant plasmid was unable to suppress like the empty vector (Fig. 6*B*).

To make sure that the mutant protein was indeed expressed and stable, we tagged with the c-Myc epitope sequence both the

wild-type and mutant *OMS1* genes carried on the high copy plasmid and measured the accumulation of the tagged protein in purified mitochondria. Western blot analysis showed that the mutation in Oms1p motif II did not modify its stability (Fig. 6*C*), thus demonstrating that the loss of the suppression was indeed due to the mutation itself and not to a lower dosage of Oms1p.

Together these results show that Oms1p methyltransferase-conserved motif II is essential for the suppression of *oxa1* mutations and strongly suggest that Oms1p is indeed a methyltransferase and that this enzymatic activity is responsible of the suppression.

DISCUSSION

The absence of Oxa1p leads to a highly pleiotropic phenotype with defects in the biogenesis of all of the respiratory complexes that contain mitochondrially encoded subunits, suggesting that Oxa1p is acting on various substrates and/or fulfills different functions. In this study, we have created point or deletion mutants in various domains of the *S. cerevisiae* Oxa1p and determined whether different roles could be assigned to the different domains. Looking at the predicted topology of Oxa1p, three main regions were present: 1) the acidic intermembrane space domain with the N-terminal end and loop L2; 2) the basic matrix domain containing the loop L1 and the C-terminal tail; and 3) the TM domains with the five hydrophobic helices.

Concerning the TM domains, TM4 and TM5 appear essential and the mutation WW→AA in or close to the TM1 domain (according to topology predictions) exhibits a stringent thermosensitive respiratory deficiency. Interestingly, this WW→AA mutant only affects cytochrome *c* oxidase. The positive charge Arg^{140} conserved in the various Oxa1p homologs and located either within or in the vicinity of TM1 as highlighted by Kuhn *et al.* (9) does not appear to be important for function. Concerning the hydrophilic domains, we have shown that L2 is essential for Oxa1p function, whereas truncations of either L1 or the C-terminal tail, which both protrude into the matrix, have no or limited consequences on respiration. However, we observed a synergistic defect when we combined the deletions of these two matrix domains. Indeed, in this double mutant ΔL1-K332*, Oxa1p, although shortened by one-third, still accumulates at the same level compared with both single mutants but the assembly of the three last respiratory complexes is now strongly affected. However, there is a substantial processing of pre-Cox2p, showing that the remaining parts of Oxa1p are still relatively efficient in mediating the insertion of pre-Cox2p N terminus into the membrane. Thus, another process must be deficient in ΔL1-K332* to explain the respiratory deficiency. Two recent papers (15, 16) have implicated the C-terminal tail of Oxa1p in contacting the translating ribosome, thereby mediating a co-translational insertion of the newly synthesized mitochondrial peptides. However the C-terminal tail truncations show a rather mild phenotype compared with the phenotype of the ΔL1-K332* strain. Szyrach *et al.* (16) have found that, despite this strong growth on glycerol, the $oxa1^{1–331}$ mutant cannot bind ribosomes *in vitro* anymore. These results could simply illustrate the difference between *in vivo* and *in vitro*, *i.e.* growth could still be obtained *in vivo* despite a low or compromised ribosome binding that becomes undetectable *in vitro*. In this case, the remaining *in vivo* ribosome binding activity of Oxa1p could be due to (i) the production of undetectably low levels of wild-type Oxa1p by readthrough from the $oxa1^{1–331}$/K332* mutant, (ii) the binding through the remaining 15 residues of the C-tail in the $oxa1^{1–331}$/K332* mutant, or (iii) cooperative action for ribosome binding through the L1 loop. Indeed the L1 loop of Oxa1p, like the C-terminal tail, displayed a positively charged coiled-coil structure (16) and could cooperate with the C-terminal tail in contacting ribosomes or translated RNAs to increase the efficiency of the insertion process.

In *E. coli*, the gene encoding the YidC homolog of Oxa1p has been mutated to study the role of the different domains and the authors concluded that none of the hydrophilic periplasmic or cytoplasmic domain residues was important for YidC activity (47). The present study as well as previous work (15, 16, 25) stressed the role of the intermembrane space loop and the matrix domains of Oxa1p for function. This difference between the bacterial and yeast proteins might be explained by the fact that YidC cooperates with the Sec system (48), whereas the Sec-type proteins are absent in yeast mitochondria (49). YidC would function merely as a hydrophobic platform receiving substrates from the Sec complex to mediate their lateral exit into the membrane while the mitochondrial Oxa1p, which exists as a homotetramer (50), would also play at least some of the various roles of the different proteins of the Sec complex.

The *oxa1* mutants have allowed the identification of a suppressor gene, *OMS1*, encoding a new mitochondrial inner membrane protein. The overexpression of *OMS1* suppresses mutations affecting various domains of Oxa1p: the loop L2 in the *ts1402* mutant; the matrix regions in ΔL1-K332*; and the TM1 segment in WW→AA. So far, nuclear-encoded suppressors able to compensate for the absence of Oxa1p have been isolated in two genes, *CYT1* and *QCR9*. Both encode integral membrane subunits of the *bc1* complex. In most cases, the suppressor mutation created a positive charge in the TM domain of these proteins (4, 46) For Cyt1-1p, the suppression is clearly driven by the short N-terminal part containing the mutated TM. It was proposed that this positively charged TM domain could compensate for the absence of Oxa1p by being co-inserted with negatively charged TM segments that are substrates of Oxa1p, similar to the first TM domain of Cox2p (4). Interestingly, the hydrophobic stretch of Oms1p was flanked by numerous positive charges, which were predicted to be part of the TM segment, and could represent a natural equivalent of the Cyt1-1p suppressor. Three lines of evidence suggest that this was not the case. First, when we attached the c-Myc epitope to the middle of the *OMS1* ORF to produce a truncated Oms1p-c-Myc containing the TM segment but lacking the methyltransferase domain, the strong suppression of the *oxa1* mutants was lost (data not shown). However, we were not able to detect the tagged truncated protein, preventing any definite conclusion to be drawn. Second, we found that Oms1p overproduction cannot compensate for the complete absence of Oxa1p, whereas Cyt1-1p does. Third and most importantly, we found that the mutation of a conserved methyltransferase motif located >200 residues downstream the TM segment abolishes the suppression. Thus, the two suppression mechanisms clearly differ. The enzymatic activity and not the TM segment appeared to be responsible for the suppression by Oms1p.

In addition, similar to *OXA1* (44) and contrary to *CYT1-1*, *OMS1* overexpression is able to compensate for the absence of the matrix protease Afg3p. This suppression can be linked to the observation that overexpression of *OMS1*, similar to the overexpression of the wild-type *OXA1* gene, increases 4-fold the steady-state level of the truncated ΔL1-K332* Oxa1p. One possibility would be that *OMS1* overexpression can stabilize not only the truncated but also the wild-type Oxa1p and thus mimics an elevated copy number of *OXA1*, thereby mediating Δ*afg3* suppression. Similarly, the increase in the steady-state level of the truncated Oxa1p when *OMS1* is overexpressed

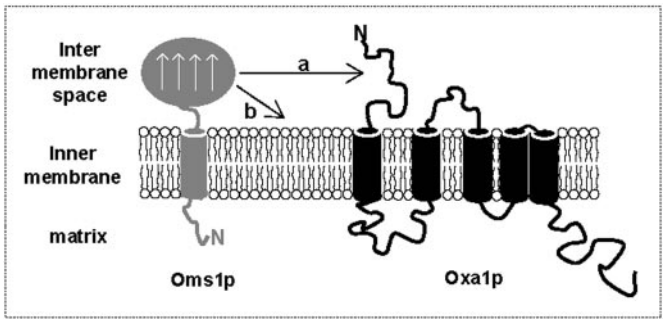

FIG. 7. **Possible mechanisms of suppression.** Oms1p is shown in *gray* tethered to inner membrane by its TM segment with its C-terminal methyltransferase domain located in the intermembrane space and containing the four conserved motifs (*white arrows*). Oxa1p is shown in *black* with its typical five TM segment N-out C-in structure. Oms1p methyltransferase activity could have for target specific residues in the intermembrane space loops of Oxa1p (*a*) or lipids within the bilayer (*b*). *N*, N terminus.

seems sufficient to explain the improved growth of the ΔL1-K332* mutant because overproduction of the truncated ΔL1-K332* protein can compensate for the complete absence of Oxa1p.

Whereas the increase of wild-type or mutant Oxa1p could account for the observed suppressions, the question remains of how these increases in steady-state levels are mediated. We observed that overexpression of wild-type *OXA1* stabilizes the mutant ΔL1-K332* protein. Because Oxa1p is known to facilitate its own insertion (37) and to exist as homotetramers (50), a reasonable hypothesis is that the wild-type Oxa1p could form a complex with the ΔL1-K332* variant and stabilize it and/or promote its membrane insertion. In the case of *OMS1* overexpression, a post-translational modification of Oxa1p by Oms1p could either increase its resistance to proteases like Oma1p (38) or freeze Oxa1p conformation after membrane insertion to enhance its stability and optimize its functioning. The methyltransferase active site of Oms1p is located in the intermembrane space, and Oms1p isoelectric point is highly basic, similar to that of the numerous methyltransferases that modify acidic substrates such as nucleic acids or phospholipids (data not shown). These observations suggest that the Oms1p substrate should be acidic and located on the external face of the inner membrane. An obvious possibility is that Oms1p methylates residues of the overall highly negatively charged N-tail or Loop 2 of Oxa1p, both of which protrude into the intermembrane space (Fig. 7). Basic residues are known to be particularly reactive substrates of protein methyltransferases. A single arginine is present in Oxa1p intermembrane space domains at position 221 close to TM2 and could be a potential target of Oms1p, but it might also be important for the initial steps of Oxa1p membrane insertion. Alternatively, Oms1p could methylate phospholipids on the external face of the mitochondrial inner membrane (Fig. 7). Indeed, some of the bacterial proteins showing a close similarity to the C-terminal domain of Oms1p encoded quinone or phospholipid methyltransferases. The modification of mitochondrial membrane lipid substrates by Oms1p could modify membrane fluidity and increase the stability of Oxa1p or its mutant derivatives and/or insertion efficiency of TM domains. Whether Oms1p acts on Oxa1p or on lipids, both hypotheses are consistent with the observation that the absence of Oms1p had only a mild effect on mitochondrial physiology but started to be deleterious when mitochondrial membrane insertion was partly defective such as in the WW→AA mutant. In addition to enlightening the mechanism of suppression, the identification of the Oms1p substrate(s) and interacting component(s), *e.g.* through a synthetic lethal screen on glycerol medium, will bring new information on its role in mitochondrial biogenesis or maintenance.

Acknowledgments—We thank F. Lacroute for the gift of the pFL44L genomic library, T. D. Fox, J. M. Galan, and J. Velours for the gift of antibodies, R. A. Stuart and K. Hell for the W303-*ts1402* strain, J. M. Herrmann for the Δ*mba1* strain, A. Tzagoloff for the Δ*afg3* strain, and M. S. Longtine for c-Myc-tagging plasmids. We thank N. Lachacinski for excellent technical assistance, J.-L. Popot and C. J. Herbert for helpful discussions, and C. J. Herbert for critical reading of the paper and grammatical corrections.

REFERENCES

1. Wiedemann, N., Frazier, A. E., and Pfanner, N. (2004) *J. Biol. Chem.* **279,** 14473–14476
2. Sanchirico, M. E., Fox, T. D., and Mason, T. L. (1998) *EMBO J.* **17,** 5796–5804
3. Bonnefoy, N., Bsat, N., and Fox, T. D. (2001) *Mol. Cell. Biol.* **21,** 2359–2372
4. Saint-Georges, Y., Hamel, P., Lemaire, C., and Dujardin, G. (2001) *Proc. Natl. Acad. Sci. U. S. A.* **98,** 13814–13819
5. Herrmann, J. M., and Bonnefoy, N. (2004) *J. Biol. Chem.* **279,** 2507–2512
6. Bonnefoy, N., Kermorgant, M., Groudinsky, O., Minet, M., Slonimski, P. P., and Dujardin, G. (1994) *Proc. Natl. Acad. Sci. U. S. A.* **91,** 11978–11982
7. Hamel, P., Sakamoto, W., Wintz, H., and Dujardin, G. (1997) *Plant J.* **12,** 1319–1327
8. Herrmann, J. M., and Neupert, W. (2003) *IUBMB Life* **55,** 219–225
9. Kuhn, A., Stuart, R., Henry, R., and Dalbey, R. E. (2003) *Trends Cell Biol.* **13,** 510–516
10. Serek, J., Bauer-Manz, G., Struhalla, G., Van Den Berg, L., Kiefer, D., Dalbey, R., and Kuhn, A. (2004) *EMBO J.* **23,** 294–301
11. Bonnefoy, N., Chalvet, F., Hamel, P., Slonimski, P. P., and Dujardin, G. (1994) *J. Mol. Biol.* **239,** 201–212
12. Altamura, N., Capitanio, N., Bonnefoy, N., Papa, S., and Dujardin, G. (1996) *FEBS Lett.* **382,** 111–115
13. He, S., and Fox, T. D. (1997) *Mol. Biol. Cell* **8,** 1449–1460
14. Hell, K., Herrmann, J., Pratje, E., Neupert, W., and Stuart, R. A. (1997) *FEBS Lett.* **418,** 367–370
15. Jia, L., Dienhart, M., Schramp, M., McCauley, M., Hell, K., and Stuart, R. A. (2003) *EMBO J.* **22,** 6438–6447
16. Szyrach, G., Ott, M., Bonnefoy, N., Neupert, W., and Herrmann, J. M. (2003) *EMBO J.* **22,** 6448–6457
17. van der Laan, M., Urbanus, M. L., Ten Hagen-Jongman, C. M., Nouwen, N., Oudega, B., Harms, N., Driessen, A. J., and Luirink, J. (2003) *Proc. Natl. Acad. Sci. U. S. A.* **100,** 5801–5806
18. van der Laan, M., Bechtluft, P., Kol, S., Nouwen, N., and Driessen, A. J. (2004) *J. Cell Biol.* **165,** 213–222
19. Yi, L., Jiang, F., Chen, M., Cain, B., Bolhuis, A., and Dalbey, R. E. (2003) *Biochemistry* **42,** 10537–10544
20. Moore, M., Goforth, R. L., Mori, H., and Henry, R. (2003) *J. Cell Biol.* **162,** 1245–1254
21. Ossenbuhl, F., Gohre, V., Meurer, J., Krieger-Liszkay, A., Rochaix, J. D., and Eichacker, L. A. (2004) *Plant Cell* **16,** 1790–1800
22. Luirink, J., Samuelsson, T., and de Gier, J. W. (2001) *FEBS Lett.* **501,** 1–5
23. Yen, M. R., Harley, K. T., Tseng, Y. H., and Saier, M. H., Jr. (2001) *FEMS Microbiol. Lett.* **204,** 223–231
24. Herrmann, J. M., Neupert, W., and Stuart, R. A. (1997) *EMBO J.* **16,** 2217–2226
25. Bauer, M., Behrens, M., Esser, K., Michaelis, G., and Pratje, E. (1994) *Mol. Gen. Genet.* **245,** 272–278
26. Sikorski, R. S., and Hieter, P. (1989) *Genetics* **122,** 19–27
27. Ho, S. N., Hunt, H. D., Horton, R. M., Pullen, J. K., and Pease, L. R. (1989) *Gene* (*Amst.*) **77,** 51–59
28. Hill, J. E., Myers, A. M., Koerner, T. J., and Tzagoloff, A. (1986) *Yeast* **2,** 163–167
29. Takata, Y., Konishi, K., Gomi, T., and Fujioka, M. (1994) *J. Biol. Chem.* **269,** 5537–5542
30. Longtine, M. S., McKenzie, A., III, Demarini, D. J., Shah, N. G., Wach, A., Brachat, A., Philippsen, P., and Pringle, J. R. (1998) *Yeast* **14,** 953–961
31. Kermorgant, M., Bonnefoy, N., and Dujardin, G. (1997) *Curr. Genet.* **31,** 302–307
32. Funes, S., Nargang, F. E., Neupert, W., and Herrmann, J. M. (2004) *Mol. Biol. Cell* **15,** 1853–1861
33. Pajot, P. (1976) *Eur. J. Biochem.* **63,** 263–269
34. Brasseur, G., Coppee, J., Colson, A.-M., and Brivet-Chevillotte, P. (1995) *J. Biol. Chem.* **270,** 29356–29364
35. Spannagel, C., Vaillier, J., Chaignepain, S., and Velours, J. (1998) *Biochemistry* **37,** 615–621
36. Lemaire, C., Hamel, P., Velours, J., and Dujardin, G. (2000) *J. Biol. Chem.* **275,** 23471–23475
37. Hell, K., Herrmann, J. M., Pratje, E., Neupert, W., and Stuart, R. A. (1998) *Proc. Natl. Acad. Sci. U. S. A.* **95,** 2250–2255
38. Kaser, M., Kambacheld, M., Kisters-Woike, B., and Langer, T. (2003) *J. Biol. Chem.* **278,** 46414–46423
39. Preuss, M., Leonhard, K., Hell, K., Stuart, R. A., Neupert, W., and Herrmann, J. M. (2001) *J. Cell Biol.* **153,** 1085–1096
40. Groudinsky, O., Bousquet, I., Wallis, M. G., Slonimski, P. P., and Dujardin, G. (1993) *Mol. Gen. Genet.* **240,** 419–427
41. Mulero, J. J., and Fox, T. D. (1994) *Mol. Gen. Genet.* **242,** 383–390
42. Bousquet, I., Dujardin, G., and Slonimski, P. P. (1991) *EMBO J.* **10,** 2023–2031
43. Niewmierzycka, A., and Clarke, S. (1999) *J. Biol. Chem.* **274,** 814–824

44. Rep, M., Nooy, J., Guelin, E., and Grivell, L. A. (1996) *Curr. Genet.* **30,** 206–211
45. Leonhard, K., Herrmann, J. M., Stuart, R. A., Mannhaupt, G., Neupert, W., and Langer, T. (1996) *EMBO J.* **15,** 4218–4229
46. Hamel, P., Lemaire, C., Bonnefoy, N., Brivet-Chevillotte, P., and Dujardin, G. (1998) *Genetics* **150,** 601–611
47. Jiang, F., Chen, M., Yi, L., de Gier, J. W., Kuhn, A., and Dalbey, R. E. (2003) *J. Biol. Chem.* **278,** 48965–48972
48. Scotti, P. A., Urbanus, M. L., Brunner, J., de Gier, J. W., von Heijne, G., van der Does, C., Driessen, A. J., Oudega, B., and Luirink, J. (2000) *EMBO J.* **19,** 542–549
49. Glick, B. S., and Von Heijne, G. (1996) *Protein Sci.* **5,** 2651–2652
50. Nargang, F. E., Preuss, M., Neupert, W., and Herrmann, J. M. (2002) *J. Biol. Chem.* **277,** 12846–12853
51. van Dyck, L., Neupert, W., and Langer, T. (1998) *Genes Dev.* **12,** 1515–1524
52. Vargas, C., McEwan, A. G., and Downie, J. A. (1993) *Anal. Biochem.* **209,** 323–326